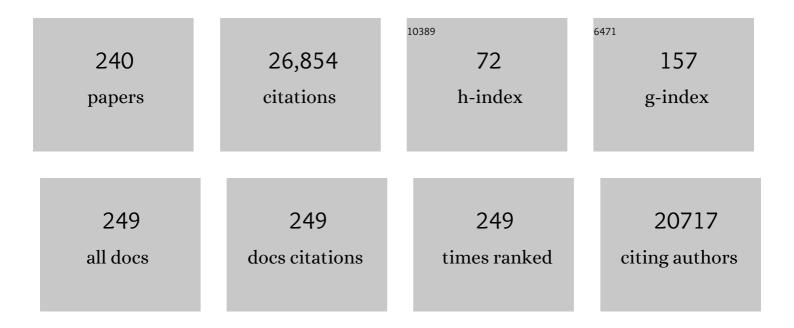
Zheng Jiang

List of Publications by Year in descending order

Source: https://exaly.com/author-pdf/2457751/publications.pdf Version: 2024-02-01



ZHENC LIANC

#	Article	IF	CITATIONS
1	Single-atom catalysis of CO oxidation using Pt1/FeOx. Nature Chemistry, 2011, 3, 634-641.	13.6	5,149
2	Low-temperature hydrogen production from water and methanol using Pt/α-MoC catalysts. Nature, 2017, 544, 80-83.	27.8	1,090
3	Electrocatalytic reduction of CO2 to ethylene and ethanol through hydrogen-assisted C–C coupling over fluorine-modified copper. Nature Catalysis, 2020, 3, 478-487.	34.4	788
4	Atomic-level insight into super-efficient electrocatalytic oxygen evolution on iron and vanadium co-doped nickel (oxy)hydroxide. Nature Communications, 2018, 9, 2885.	12.8	669
5	High performance platinum single atom electrocatalyst for oxygen reduction reaction. Nature Communications, 2017, 8, 15938.	12.8	569
6	An Isolated Zinc–Cobalt Atomic Pair for Highly Active and Durable Oxygen Reduction. Angewandte Chemie - International Edition, 2019, 58, 2622-2626.	13.8	494
7	Chemically activating MoS2 via spontaneous atomic palladium interfacial doping towards efficient hydrogen evolution. Nature Communications, 2018, 9, 2120.	12.8	461
8	Promoting electrocatalytic CO2 reduction to formate via sulfur-boosting water activation on indium surfaces. Nature Communications, 2019, 10, 892.	12.8	446
9	Climbing the Apex of the ORR Volcano Plot via Binuclear Site Construction: Electronic and Geometric Engineering. Journal of the American Chemical Society, 2019, 141, 17763-17770.	13.7	436
10	Single-Atomic Ruthenium Catalytic Sites on Nitrogen-Doped Graphene for Oxygen Reduction Reaction in Acidic Medium. ACS Nano, 2017, 11, 6930-6941.	14.6	435
11	Microporous Framework Induced Synthesis of Single-Atom Dispersed Fe-N-C Acidic ORR Catalyst and Its in Situ Reduced Fe-N ₄ Active Site Identification Revealed by X-ray Absorption Spectroscopy. ACS Catalysis, 2018, 8, 2824-2832.	11.2	433
12	Dynamic oxygen adsorption on single-atomic Ruthenium catalyst with high performance for acidic oxygen evolution reaction. Nature Communications, 2019, 10, 4849.	12.8	416
13	Chromium-ruthenium oxide solid solution electrocatalyst for highly efficient oxygen evolution reaction in acidic media. Nature Communications, 2019, 10, 162.	12.8	396
14	C and N Hybrid Coordination Derived Co–C–N Complex as a Highly Efficient Electrocatalyst for Hydrogen Evolution Reaction. Journal of the American Chemical Society, 2015, 137, 15070-15073.	13.7	377
15	Highly Efficient CO ₂ Electroreduction on ZnN ₄ â€based Singleâ€Atom Catalyst. Angewandte Chemie - International Edition, 2018, 57, 12303-12307.	13.8	356
16	In-situ reconstructed Ru atom array on α-MnO2 with enhanced performance for acidic water oxidation. Nature Catalysis, 2021, 4, 1012-1023.	34.4	324
17	Identification of binuclear Co2N5 active sites for oxygen reduction reaction with more than one magnitude higher activity than single atom CoN4 site. Nano Energy, 2018, 46, 396-403.	16.0	319
18	Singleâ€Atom Crâ^'N ₄ Sites Designed for Durable Oxygen Reduction Catalysis in Acid Media. Angewandte Chemie - International Edition, 2019, 58, 12469-12475.	13.8	307

#	Article	IF	CITATIONS
19	Synergistic Effect between Metal–Nitrogen–Carbon Sheets and NiO Nanoparticles for Enhanced Electrochemical Waterâ€Oxidation Performance. Angewandte Chemie - International Edition, 2015, 54, 10530-10534.	13.8	301
20	Zn Single Atom Catalyst for Highly Efficient Oxygen Reduction Reaction. Advanced Functional Materials, 2017, 27, 1700802.	14.9	296
21	A highly CO-tolerant atomically dispersed Pt catalyst for chemoselective hydrogenation. Nature Nanotechnology, 2019, 14, 354-361.	31.5	292
22	A stable low-temperature H2-production catalyst by crowding Pt on $\hat{I}\pm$ -MoC. Nature, 2021, 589, 396-401.	27.8	290
23	An Engineered Superhydrophilic/Superaerophobic Electrocatalyst Composed of the Supported CoMoS _{<i>x</i>} Chalcogel for Overall Water Splitting. Angewandte Chemie - International Edition, 2020, 59, 1659-1665.	13.8	268
24	Carbon‣upported Divacancyâ€Anchored Platinum Singleâ€Atom Electrocatalysts with Superhigh Pt Utilization for the Oxygen Reduction Reaction. Angewandte Chemie - International Edition, 2019, 58, 1163-1167.	13.8	252
25	Manipulating spin polarization of titanium dioxide for efficient photocatalysis. Nature Communications, 2020, 11, 418.	12.8	252
26	Lithiation-induced amorphization of Pd3P2S8 for highly efficient hydrogen evolution. Nature Catalysis, 2018, 1, 460-468.	34.4	247
27	Generating Defectâ€Rich Bismuth for Enhancing the Rate of Nitrogen Electroreduction to Ammonia. Angewandte Chemie - International Edition, 2019, 58, 9464-9469.	13.8	226
28	Iron Vacancies Induced Bifunctionality in Ultrathin Feroxyhyte Nanosheets for Overall Water Splitting. Advanced Materials, 2018, 30, e1803144.	21.0	225
29	Anchoring Cu1 species over nanodiamond-graphene for semi-hydrogenation of acetylene. Nature Communications, 2019, 10, 4431.	12.8	224
30	Enhanced Photocatalytic Activity and Electron Transfer Mechanisms of Graphene/TiO ₂ with Exposed {001} Facets. Journal of Physical Chemistry C, 2011, 115, 23718-23725.	3.1	223
31	Subnanometer Bimetallic Platinum–Zinc Clusters in Zeolites for Propane Dehydrogenation. Angewandte Chemie - International Edition, 2020, 59, 19450-19459.	13.8	221
32	Synergistic Doping and Intercalation: Realizing Deep Phase Modulation on MoS ₂ Arrays for Highâ€Efficiency Hydrogen Evolution Reaction. Angewandte Chemie - International Edition, 2019, 58, 16289-16296.	13.8	201
33	An In Situ Formed Surface Coating Layer Enabling LiCoO ₂ with Stable 4.6 V Highâ€Voltage Cycle Performances. Advanced Energy Materials, 2020, 10, 2001413.	19.5	201
34	Fluorination-enabled Reconstruction of NiFe Electrocatalysts for Efficient Water Oxidation. Nano Letters, 2021, 21, 492-499.	9.1	190
35	Visible light-driven Câ^'H activation and C–C coupling of methanol into ethylene glycol. Nature Communications, 2018, 9, 1181.	12.8	188
36	Carbide-Supported Au Catalysts for Water–Gas Shift Reactions: A New Territory for the Strong Metal–Support Interaction Effect. Journal of the American Chemical Society, 2018, 140, 13808-13816.	13.7	188

#	Article	IF	CITATIONS
37	Confined small-sized cobalt catalysts stimulate carbon-chain growth reversely by modifying ASF law of Fischer–Tropsch synthesis. Nature Communications, 2018, 9, 3250.	12.8	186
38	Rational construction of oxygen vacancies onto tungsten trioxide to improve visible light photocatalytic water oxidation reaction. Applied Catalysis B: Environmental, 2018, 239, 398-407.	20.2	183
39	Confined Ir single sites with triggered lattice oxygen redox: Toward boosted and sustained water oxidation catalysis. Joule, 2021, 5, 2164-2176.	24.0	183
40	Highâ€Valence Nickel Singleâ€Atom Catalysts Coordinated to Oxygen Sites for Extraordinarily Activating Oxygen Evolution Reaction. Advanced Science, 2020, 7, 1903089.	11.2	182
41	Insights into the effects of surface/bulk defects on photocatalytic hydrogen evolution over TiO2 with exposed {001} facets. Applied Catalysis B: Environmental, 2018, 220, 126-136.	20.2	176
42	Bridge Bonded Oxygen Ligands between Approximated FeN ₄ Sites Confer Catalysts with High ORR Performance. Angewandte Chemie - International Edition, 2020, 59, 13923-13928.	13.8	176
43	Weak magnetic field significantly enhances selenite removal kinetics by zero valent iron. Water Research, 2014, 49, 371-380.	11.3	172
44	Atomically Dispersed Ni/α-MoC Catalyst for Hydrogen Production from Methanol/Water. Journal of the American Chemical Society, 2021, 143, 309-317.	13.7	168
45	Insight into the Formation of Co@Co ₂ C Catalysts for Direct Synthesis of Higher Alcohols and Olefins from Syngas. ACS Catalysis, 2018, 8, 228-241.	11.2	152
46	Tin-Assisted Fully Exposed Platinum Clusters Stabilized on Defect-Rich Graphene for Dehydrogenation Reaction. ACS Catalysis, 2019, 9, 5998-6005.	11.2	150
47	Ag-Incorporated Organic–Inorganic Perovskite Films and Planar Heterojunction Solar Cells. Nano Letters, 2017, 17, 3231-3237.	9.1	149
48	Oxygen Vacancy Tuning toward Efficient Electrocatalytic CO ₂ Reduction to C ₂ H ₄ . Small Methods, 2019, 3, 1800449.	8.6	146
49	Comprehensive Understanding of the Spatial Configurations of CeO ₂ in NiO for the Electrocatalytic Oxygen Evolution Reaction: Embedded or Surfaceâ€Loaded. Advanced Functional Materials, 2018, 28, 1706056.	14.9	141
50	Simultaneous oxidative and reductive reactions in one system by atomic design. Nature Catalysis, 2021, 4, 134-143.	34.4	132
51	Single atom dispersed Rh-biphephos&PPh ₃ @porous organic copolymers: highly efficient catalysts for continuous fixed-bed hydroformylation of propene. Green Chemistry, 2016, 18, 2995-3005.	9.0	127
52	Graphitic phosphorus coordinated single Fe atoms for hydrogenative transformations. Nature Communications, 2020, 11, 4074.	12.8	122
53	Wavelet analysis of extended X-ray absorption fine structure data: Theory, application. Physica B: Condensed Matter, 2018, 542, 12-19.	2.7	114
54	Covalent Triazine Framework Confined Copper Catalysts for Selective Electrochemical CO ₂ Reduction: Operando Diagnosis of Active Sites. ACS Catalysis, 2020, 10, 4534-4542.	11.2	112

#	Article	IF	CITATIONS
55	Adsorption Site Regulation to Guide Atomic Design of Ni–Ga Catalysts for Acetylene Semiâ€Hydrogenation. Angewandte Chemie - International Edition, 2020, 59, 11647-11652.	13.8	111
56	Regulating coordination number in atomically dispersed Pt species on defect-rich graphene for n-butane dehydrogenation reaction. Nature Communications, 2021, 12, 2664.	12.8	111
57	Two-Step Carbothermal Welding To Access Atomically Dispersed Pd ₁ on Three-Dimensional Zirconia Nanonet for Direct Indole Synthesis. Journal of the American Chemical Society, 2019, 141, 10590-10594.	13.7	108
58	Reactant friendly hydrogen evolution interface based on di-anionic MoS2 surface. Nature Communications, 2020, 11, 1116.	12.8	108
59	In Situ Formation of Disorder-Engineered TiO ₂ (B)-Anatase Heterophase Junction for Enhanced Photocatalytic Hydrogen Evolution. ACS Applied Materials & Interfaces, 2015, 7, 24987-24992.	8.0	103
60	Accelerated active phase transformation of NiO powered by Pt single atoms for enhanced oxygen evolution reaction. Chemical Science, 2018, 9, 6803-6812.	7.4	96
61	Research Progress on the Indirect Hydrogenation of Carbon Dioxide to Methanol. ChemSusChem, 2016, 9, 322-332.	6.8	90
62	Atomic‣evel Feâ€Nâ€C Coupled with Fe ₃ Câ€Fe Nanocomposites in Carbon Matrixes as Highâ€Efficiency Bifunctional Oxygen Catalysts. Small, 2020, 16, e1906057.	10.0	90
63	De-NOx in alternative lean/rich atmospheres on La1â^'xSrxCoO3 perovskites. Energy and Environmental Science, 2011, 4, 3351.	30.8	87
64	Understanding oxygen vacancies in disorder-engineered surface and subsurface of CaTiO3 nanosheets on photocatalytic hydrogen evolution. Applied Catalysis B: Environmental, 2020, 267, 118378.	20.2	86
65	Highly Efficient CO ₂ Electroreduction on ZnN ₄ â€based Singleâ€Atom Catalyst. Angewandte Chemie, 2018, 130, 12483-12487.	2.0	83
66	Sequestration of Antimonite by Zerovalent Iron: Using Weak Magnetic Field Effects to Enhance Performance and Characterize Reaction Mechanisms. Environmental Science & Technology, 2016, 50, 1483-1491.	10.0	81
67	In situ tuning of electronic structure of catalysts using controllable hydrogen spillover for enhanced selectivity. Nature Communications, 2020, 11, 4773.	12.8	81
68	Highly Ethylene‧elective Electrocatalytic CO ₂ Reduction Enabled by Isolated Cuâ^'S Motifs in Metal–Organic Framework Based Precatalysts. Angewandte Chemie - International Edition, 2022, 61, .	13.8	81
69	COâ€Tolerant PEMFC Anodes Enabled by Synergistic Catalysis between Iridium Singleâ€Atom Sites and Nanoparticles. Angewandte Chemie - International Edition, 2021, 60, 26177-26183.	13.8	81
70	High-loaded sub-6 nm Pt1Co1 intermetallic compounds with highly efficient performance expression in PEMFCs. Energy and Environmental Science, 2022, 15, 278-286.	30.8	81
71	Direct Methylation of Amines with Carbon Dioxide and Molecular Hydrogen using Supported Gold Catalysts. ChemSusChem, 2015, 8, 3489-3496.	6.8	80
72	Trifunctional C@MnO Catalyst for Enhanced Stable Simultaneously Catalytic Removal of Formaldehyde and Ozone. ACS Catalysis, 2018, 8, 3164-3180.	11.2	80

#	Article	IF	CITATIONS
73	Identifying Oxygen Activation/Oxidation Sites for Efficient Soot Combustion over Silver Catalysts Interacted with Nanoflower-Like Hydrotalcite-Derived CoAlO Metal Oxides. ACS Catalysis, 2019, 9, 8772-8784.	11.2	77
74	Optimizing Electron Densities of Niâ€N Complexes by Hybrid Coordination for Efficient Electrocatalytic CO ₂ Reduction. ChemSusChem, 2020, 13, 929-937.	6.8	76
75	Microwave-assisted synthesis of photoluminescent glutathione-capped Au/Ag nanoclusters: A unique sensor-on-a-nanoparticle for metal ions, anions, and small molecules. Nano Research, 2015, 8, 2329-2339.	10.4	75
76	Stabilization of Palladium Nanoparticles on Nanodiamond–Graphene Core–Shell Supports for CO Oxidation. Angewandte Chemie - International Edition, 2015, 54, 15823-15826.	13.8	74
77	In situ directional formation of Co@CoO _x -embedded 1D carbon nanotubes as an efficient oxygen electrocatalyst for ultra-high rate Zn–air batteries. Journal of Materials Chemistry A, 2017, 5, 13994-14002.	10.3	74
78	Carbon‣upported Divacancyâ€Anchored Platinum Singleâ€Atom Electrocatalysts with Superhigh Pt Utilization for the Oxygen Reduction Reaction. Angewandte Chemie, 2019, 131, 1175-1179.	2.0	73
79	Low Temperature Oxidation of Ethane to Oxygenates by Oxygen over Iridium-Cluster Catalysts. Journal of the American Chemical Society, 2019, 141, 18921-18925.	13.7	72
80	Few-Atom Pt Ensembles Enable Efficient Catalytic Cyclohexane Dehydrogenation for Hydrogen Production. Journal of the American Chemical Society, 2022, 144, 3535-3542.	13.7	72
81	Palladium single atoms supported by interwoven carbon nanotube and manganese oxide nanowire networks for enhanced electrocatalysis. Journal of Materials Chemistry A, 2018, 6, 23366-23377.	10.3	68
82	Overwhelming the Performance of Single Atoms with Atomic Clusters for Platinum-Catalyzed Hydrogen Evolution. ACS Catalysis, 2019, 9, 8213-8223.	11.2	68
83	Conjugated Covalent Organic Frameworks as Platinum Nanoparticle Supports for Catalyzing the Oxygen Reduction Reaction. Chemistry of Materials, 2020, 32, 9747-9752.	6.7	68
84	Hydrogenated Cagelike Titania Hollow Spherical Photocatalysts for Hydrogen Evolution under Simulated Solar Light Irradiation. ACS Applied Materials & Interfaces, 2016, 8, 23006-23014.	8.0	67
85	Constructing Mononuclear Palladium Catalysts by Precoordination/Solvothermal Polymerization: Recyclable Catalyst for Regioselective Oxidative Heck Reactions. Angewandte Chemie - International Edition, 2019, 58, 2448-2453.	13.8	64
86	A general synthetic approach for hexagonal phase tungsten nitride composites and their application in the hydrogen evolution reaction. Journal of Materials Chemistry A, 2018, 6, 10967-10975.	10.3	62
87	A Superlattice-Stabilized Layered CuS Anode for High-Performance Aqueous Zinc-Ion Batteries. ACS Nano, 2021, 15, 17748-17756.	14.6	62
88	Ring-Opening Transformation of 5-Hydroxymethylfurfural Using a Golden Single-Atomic-Site Palladium Catalyst. ACS Catalysis, 2019, 9, 6212-6222.	11.2	60
89	Sub-nanometric Manganous Oxide Clusters in Nitrogen Doped Mesoporous Carbon Nanosheets for High-Performance Lithium–Sulfur Batteries. Nano Letters, 2021, 21, 700-708.	9.1	60
90	Tuning interaction between cobalt catalysts and nitrogen dopants in carbon nanospheres to promote Fischer-Tropsch synthesis. Applied Catalysis B: Environmental, 2019, 248, 73-83.	20.2	58

#	Article	IF	CITATIONS
91	Understanding the Local and Electronic Structures toward Enhanced Thermal Stable Luminescence of CaAlSiN ₃ :Eu ²⁺ . Chemistry of Materials, 2016, 28, 5505-5515.	6.7	57
92	Carbon vacancy defect-activated Pt cluster for hydrogen generation. Journal of Materials Chemistry A, 2019, 7, 15364-15370.	10.3	57
93	In situ formation of mononuclear complexes by reaction-induced atomic dispersion of supported noble metal nanoparticles. Nature Communications, 2019, 10, 5281.	12.8	57
94	Achieving efficient and robust catalytic reforming on dual-sites of Cu species. Chemical Science, 2019, 10, 2578-2584.	7.4	56
95	Defect Engineering in Polymeric Cobalt Phthalocyanine Networks for Enhanced Electrochemical CO ₂ Reduction. ChemElectroChem, 2018, 5, 2717-2721.	3.4	52
96	Atomic Design and Fine-Tuning of Subnanometric Pt Catalysts to Tame Hydrogen Generation. ACS Catalysis, 2021, 11, 4146-4156.	11.2	52
97	Highly Active Graphene Oxide-Supported Cobalt Single-Ion Catalyst for Chemiluminescence Reaction. Analytical Chemistry, 2017, 89, 13518-13523.	6.5	51
98	Cooperative Sites in Fully Exposed Pd Clusters for Low-Temperature Direct Dehydrogenation Reaction. ACS Catalysis, 2021, 11, 11469-11477.	11.2	51
99	Selective methane electrosynthesis enabled by a hydrophobic carbon coated copper core–shell architecture. Energy and Environmental Science, 2022, 15, 234-243.	30.8	51
100	Achieving an exceptionally high loading of isolated cobalt single atoms on a porous carbon matrix for efficient visible-light-driven photocatalytic hydrogen production. Chemical Science, 2019, 10, 2585-2591.	7.4	50
101	Interfacial-confined coordination to single-atom nanotherapeutics. Nature Communications, 2022, 13, 91.	12.8	49
102	Generating Defectâ€Rich Bismuth for Enhancing the Rate of Nitrogen Electroreduction to Ammonia. Angewandte Chemie, 2019, 131, 9564-9569.	2.0	47
103	Subnanometer Bimetallic Platinum–Zinc Clusters in Zeolites for Propane Dehydrogenation. Angewandte Chemie, 2020, 132, 19618-19627.	2.0	47
104	Constructing Synergistic Znâ€N ₄ and Feâ€N ₄ O Dualâ€5ites from the COF@MOF Derived Hollow Carbon for Oxygen Reduction Reaction. Small Structures, 2022, 3, .	12.0	46
105	An active, selective, and stable manganese oxide-supported atomic Pd catalyst for aerobic oxidation of 5-hydroxymethylfurfural. Green Chemistry, 2019, 21, 4194-4203.	9.0	45
106	Particle Size Effects of Cobalt Carbide for Fischer–Tropsch to Olefins. ACS Catalysis, 2019, 9, 798-809.	11.2	45
107	Enhanced hydrogen generation by reverse spillover effects over bicomponent catalysts. Nature Communications, 2022, 13, 118.	12.8	44
108	A Magnetically Separable Pd Singleâ€Atom Catalyst for Efficient Selective Hydrogenation of Phenylacetylene. Advanced Materials, 2022, 34, e2110455.	21.0	44

#	Article	IF	CITATIONS
109	Grafting nanometer metal/oxide interface towards enhanced low-temperature acetylene semi-hydrogenation. Nature Communications, 2021, 12, 5770.	12.8	43
110	Confining single Pt atoms from Pt clusters on multi-armed CdS for enhanced photocatalytic hydrogen evolution. Journal of Materials Chemistry A, 2022, 10, 4594-4600.	10.3	43
111	Unravelling the Role of the Compressed Gas on Melting Point of Liquid Confined in Nanospace. Journal of Physical Chemistry Letters, 2012, 3, 1052-1055.	4.6	42
112	Selectivity Regulation in Au-Catalyzed Nitroaromatic Hydrogenation by Anchoring Single-Site Metal Oxide Promoters. ACS Catalysis, 2020, 10, 2837-2844.	11.2	42
113	A fully-conjugated covalent organic framework-derived carbon supporting ultra-close single atom sites for ORR. Applied Catalysis B: Environmental, 2022, 307, 121147.	20.2	42
114	Biocompatible Ruthenium Single-Atom Catalyst for Cascade Enzyme-Mimicking Therapy. ACS Applied Materials & Interfaces, 2021, 13, 45269-45278.	8.0	41
115	On-surface manipulation of atom substitution between cobalt phthalocyanine and the Cu(111) substrate. RSC Advances, 2017, 7, 13827-13835.	3.6	40
116	Bridge Bonded Oxygen Ligands between Approximated FeN ₄ Sites Confer Catalysts with High ORR Performance. Angewandte Chemie, 2020, 132, 14027-14032.	2.0	40
117	Planar substrate-binding site dictates the specificity of ECF-type nickel/cobalt transporters. Cell Research, 2014, 24, 267-277.	12.0	39
118	Low-Temperature Growth of Bismuth Thin Films with (111) Facet on Highly Oriented Pyrolytic Graphite. ACS Applied Materials & Interfaces, 2015, 7, 8525-8532.	8.0	39
119	Heat treated carbon supported iron(<scp>ii</scp>)phthalocyanine oxygen reduction catalysts: elucidation of the structure–activity relationship using X-ray absorption spectroscopy. Physical Chemistry Chemical Physics, 2016, 18, 33142-33151.	2.8	39
120	Promoted alkaline hydrogen evolution by an N-doped Pt–Ru single atom alloy. Journal of Materials Chemistry A, 2021, 9, 14941-14947.	10.3	39
121	Synergistic Engineering of Sulfur Vacancies and Heterointerfaces in Copper Sulfide Anodes for Aqueous Znâ€Ion Batteries with Fast Diffusion Kinetics and an Ultralong Lifespan. Advanced Energy Materials, 2022, 12, .	19.5	39
122	Interface interaction induced oxygen activation of cactus-like Co3O4/OMS-2 nanorod catalysts in situ grown on monolithic cordierite for diesel soot combustion. Applied Catalysis B: Environmental, 2021, 286, 119932.	20.2	38
123	Surface oxygen vacancies promoted Pt redispersion to single-atoms for enhanced photocatalytic hydrogen evolution. Journal of Materials Chemistry A, 2021, 9, 13890-13897.	10.3	38
124	Cu single-atoms embedded in porous carbon nitride for selective oxidation of methane to oxygenates. Chemical Communications, 2020, 56, 14677-14680.	4.1	37
125	Ru single atoms for efficient chemoselective hydrogenation of nitrobenzene to azoxybenzene. Green Chemistry, 2021, 23, 4753-4761.	9.0	35
126	High-voltage asymmetric metal–air batteries based on polymeric single-Zn2+-ion conductor. Matter, 2021, 4, 1287-1304.	10.0	34

#	Article	IF	CITATIONS
127	A Universal Singleâ€Atom Coating Strategy Based on Tannic Acid Chemistry for Multifunctional Heterogeneous Catalysis. Angewandte Chemie - International Edition, 2022, 61, .	13.8	34
128	Valence change of europium in <mml:math <br="" xmlns:mml="http://www.w3.org/1998/Math/MathML">display="inline"><mml:mrow><mml:msub><mml:mrow><mml:mtext>EuFe</mml:mtext></mml:mrow><mml:mrow compressed<mml:math display="inline" xmlns:mml="http://www.w3.org/1998/Math/MathML"><mml:mro Physical Review B, 2010, 82, .</mml:mro </mml:math></mml:mrow </mml:msub></mml:mrow></mml:math>	n>23.2	:mŋʒ
129	Hierarchical confinement of PtZn alloy nanoparticles and single-dispersed Zn atoms on COF@MOF-derived carbon towards efficient oxygen reduction reaction. Journal of Materials Chemistry A, 2021, 9, 13625-13630.	10.3	33
130	Highly Selective Acetylene Semihydrogenation Catalyst with an Operation Window Exceeding 150 °C. ACS Catalysis, 2021, 11, 6073-6080.	11.2	33
131	Fabrication of NiSe2 by direct selenylation of a nickel surface. Applied Surface Science, 2018, 428, 623-629.	6.1	33
132	Proton exchange membrane fuel cells powered with both CO and H ₂ . Proceedings of the National Academy of Sciences of the United States of America, 2021, 118, .	7.1	33
133	In Situ-Activated Indium Nanoelectrocatalysts for Highly Active and Selective CO ₂ Electroreduction around the Thermodynamic Potential. ACS Catalysis, 2022, 12, 8601-8609.	11.2	33
134	Oneâ€₽ot Approach to a Highly Robust Iron Oxide/Reduced Graphene Oxide Nanocatalyst for Fischer–Tropsch Synthesis. ChemCatChem, 2013, 5, 714-719.	3.7	32
135	Addition of Pd on La _{0.7} Sr _{0.3} CoO ₃ Perovskite To Enhance Catalytic Removal of NO _{<i>x</i>} . Industrial & Engineering Chemistry Research, 2018, 57, 521-531.	3.7	32
136	Construction of defect-engineered three-dimensionally ordered macroporous WO ₃ for efficient photocatalytic water oxidation reaction. Journal of Materials Chemistry A, 2021, 9, 3036-3043.	10.3	32
137	Defective C3N4 frameworks coordinated diatomic copper catalyst: Towards mild oxidation of methane to C1 oxygenates. Applied Catalysis B: Environmental, 2021, 299, 120682.	20.2	32
138	Pt/Fe ₃ O ₄ Core/Shell Triangular Nanoprisms by Heteroepitaxy: Facet Selectivity at the Pt–Fe ₃ O ₄ Interface and the Fe ₃ O ₄ Outer Surface. ACS Nano, 2015, 9, 10950-10960.	14.6	31
139	Modification of Cu/SiO ₂ Catalysts by La ₂ O ₃ to Quantitatively Tune Cu ⁺ u ⁰ Dual Sites with Improved Catalytic Activities and Stabilities for Dimethyl Ether Steam Reforming. ChemCatChem, 2018, 10, 3862-3871.	3.7	31
140	Characterization of CoMn catalyst by in situ X-ray absorption spectroscopy and wavelet analysis for Fischer–Tropsch to olefins reaction. Journal of Energy Chemistry, 2019, 32, 118-123.	12.9	31
141	Dopamine sacrificial coating strategy driving formation of highly active surface-exposed Ru sites on Ru/TiO2 catalysts in Fischer–Tropsch synthesis. Applied Catalysis B: Environmental, 2020, 278, 119261.	20.2	31
142	Adsorption Site Regulation to Guide Atomic Design of Ni–Ga Catalysts for Acetylene Semiâ€Hydrogenation. Angewandte Chemie, 2020, 132, 11744-11749.	2.0	31
143	Cu3(PO4)2/C composite as a high-capacity cathode material for rechargeable Na-ion batteries. Nano Energy, 2016, 27, 420-429.	16.0	30
144	Uniform Pt quantum dots-decorated porous g-C3N4 nanosheets for efficient separation of electron-hole and enhanced solar-driven photocatalytic performance. Journal of Colloid and Interface Science, 2018, 531, 119-125.	9.4	30

#	Article	IF	CITATIONS
145	Increasing the activity and selectivity of Co-based FTS catalysts supported by carbon materials for direct synthesis of clean fuels by the addition of chromium. Journal of Catalysis, 2019, 370, 251-264.	6.2	30
146	Singleâ€Atom Crâ^'N ₄ Sites Designed for Durable Oxygen Reduction Catalysis in Acid Media. Angewandte Chemie, 2019, 131, 12599-12605.	2.0	29
147	Rational design of edges of covalent organic networks for catalyzing hydrogen peroxide production. Applied Catalysis B: Environmental, 2021, 298, 120605.	20.2	29
148	Compression of ionic liquid when confined in porous silica nanoparticles. RSC Advances, 2013, 3, 9618.	3.6	27
149	Operando HERFD-XANES and surface sensitive Δμ analyses identify the structural evolution of copper(II) phthalocyanine for electroreduction of CO2. Journal of Energy Chemistry, 2022, 64, 1-7.	12.9	27
150	Tandem Catalysis for Selective Oxidation of Methane to Oxygenates Using Oxygen over PdCu/Zeolite. Angewandte Chemie - International Edition, 2022, 61, .	13.8	27
151	Elemental depth profile of faux bamboo paint in Forbidden City studied by synchrotron radiation confocal µâ€XRF. X-Ray Spectrometry, 2008, 37, 595-598.	1.4	26
152	Pressure-induced quantum phase transitions in a <mml:math xmlns:mml="http://www.w3.org/1998/Math/MathML"><mml:mrow><mml:mi>Yb</mml:mi><mml:msub><mml:mi mathvariant="normal">B<mml:mn>6</mml:mn></mml:mi </mml:msub></mml:mrow>single crystal. Physical Review B, 2015, 92, .</mml:math 	i _{3.2}	26
153	Dual″onically Bound Single‣ite Rhodium on Porous Ionic Polymer Rivals Commercial Methanol Carbonylation Catalysts. Advanced Materials, 2019, 31, e1904976.	21.0	26
154	2D-organic framework confined metal single atoms with the loading reaching the theoretical limit. Materials Horizons, 2020, 7, 2726-2733.	12.2	26
155	High urie <i>â€</i> Temperature Ferromagnetism in (Sc,Fe)F ₃ Fluorides and its Dependence on Chemical Valence. Advanced Materials, 2015, 27, 4592-4596.	21.0	25
156	Local structure study of tellurium corrosion of nickel alloy by X-ray absorption spectroscopy. Corrosion Science, 2016, 108, 169-172.	6.6	25
157	Electronic Structure and Photoluminescence Origin of Single-Crystalline Germanium Oxide Nanowires with Green Light Emission. Journal of Physical Chemistry C, 2011, 115, 11420-11426.	3.1	24
158	Effect of different synthetic routes on the performance of propylene hydroformylation over 3V-PPh3 polymer supported Rh catalysts. Reaction Kinetics, Mechanisms and Catalysis, 2015, 116, 223-234.	1.7	23
159	Fabricating Quasi-Free-Standing Graphene on a SiC(0001) Surface by Steerable Intercalation of Iron. Journal of Physical Chemistry C, 2018, 122, 21484-21492.	3.1	23
160	lodide-Coordinated Single-Site Pd Catalysts for Alkyne Dialkoxycarbonylation. ACS Catalysis, 2021, 11, 9242-9251.	11.2	23
161	Antisintering Pd ₁ Catalyst for Propane Direct Dehydrogenation with In Situ Active Sites Regeneration Ability. ACS Catalysis, 2022, 12, 2244-2252.	11.2	23
162	Introducing Co–O Moiety to Co–N–C Single-Atom Catalyst for Ethylbenzene Dehydrogenation. ACS Catalysis, 2022, 12, 7760-7772.	11.2	23

#	Article	IF	CITATIONS
163	CoN ₅ Sites Constructed by Anchoring Co Porphyrins on Vinyleneâ€Linked Covalent Organic Frameworks for Electroreduction of Carbon Dioxide. Small, 2022, 18, .	10.0	23
164	Temperature-Induced Molecular Rearrangement of an Ionic Liquid Confined in Nanospaces: An <i>in Situ</i> X-ray Absorption Fine Structure Study. Journal of Physical Chemistry C, 2015, 119, 22724-22731.	3.1	22
165	Feroxyhyte Nanosheets: Iron Vacancies Induced Bifunctionality in Ultrathin Feroxyhyte Nanosheets for Overall Water Splitting (Adv. Mater. 36/2018). Advanced Materials, 2018, 30, 1870272.	21.0	22
166	Probe active sites of heterogeneous electrocatalysts by X-ray absorption spectroscopy: From single atom to complex multi-element composites. Current Opinion in Electrochemistry, 2019, 14, 7-15.	4.8	22
167	Ni ₂ O ₃ –Au ⁺ hybrid active sites on NiO _x @Au ensembles for low-temperature gas-phase oxidation of alcohols. Catalysis Science and Technology, 2013, 3, 404-408.	4.1	21
168	Role of ReOx Species in Ni-Re/Al2O3 Catalyst for Amination of Monoethanolamine. Journal of Physical Chemistry C, 2018, 122, 23011-23025.	3.1	21
169	Highly efficient NOx purification in alternating lean/rich atmospheres over non-platinic mesoporous perovskite-based catalyst K/LaCoO3. Catalysis Science and Technology, 2013, 3, 1915.	4.1	20
170	Insight into Copper Oxideâ€Tin Oxide Catalysts for the Catalytic Oxidation of Carbon Monoxide: Identification of Active Copper Species and a Reaction Mechanism. ChemCatChem, 2017, 9, 3226-3235.	3.7	20
171	Identifying the convergent reaction path from predesigned assembled structures: Dissymmetrical dehalogenation of Br2Py on Ag(111). Nano Research, 0, , 1.	10.4	20
172	The influence of substituting metals (Ti, V, Cr, Mn, Co and Ni) on the thermal stability of magnetite. Journal of Thermal Analysis and Calorimetry, 2013, 111, 1317-1324.	3.6	19
173	Boosting Photocatalytic Water Oxidation Over Bifunctional Rh ⁰ â€Rh ³⁺ Sites. Angewandte Chemie - International Edition, 2021, 60, 22761-22768.	13.8	19
174	Low temperature surface oxygen activation in crystalline MnO2 triggered by lattice confined Pd single atoms. Journal of Energy Chemistry, 2021, 62, 136-144.	12.9	19
175	Constructing Efficient Single Rh Sites on Activated Carbon via Surface Carbonyl Groups for Methanol Carbonylation. ACS Catalysis, 2021, 11, 682-690. Local structures around (mml:math	11.2	19
176	xmlns:mml="http://www.w3.org/1998/Math/MathML"> <mml:mn>3</mml:mn> <mml:mi>d</mml:mi> dopants in topological insulator <mml:math xmlns:mml="http://www.w3.org/1998/Math/MathML"><mml:msub><mml:mrow><mml:mi mathvariant="normal">Bi</mml:mi </mml:mrow><mml:mn>2</mml:mn></mml:msub><mml:msub><mml:msub><mml:msub><mml:mrow></mml:mrow></mml:msub></mml:msub></mml:msub></mml:math 	3.2	18
177	mathvariant="normal">Se <mml:mn>3</mml:mn> studied <i>In situ</i> XAFS study on the formation process of cobalt carbide by Fischerâ€"Tropsch reaction. Physical Chemistry Chemical Physics, 2019, 21, 10791-10797.	2.8	18
178	Molecular-level insights into the electronic effects in platinum-catalyzed carbon monoxide oxidation. Nature Communications, 2021, 12, 6888.	12.8	18
179	Synergistic Doping and Intercalation: Realizing Deep Phase Modulation on MoS 2 Arrays for Highâ€Efficiency Hydrogen Evolution Reaction. Angewandte Chemie, 2019, 131, 16435-16442.	2.0	16
180	Unraveling the Potential-Dependent Volcanic Selectivity Changes of an Atomically Dispersed Ni Catalyst During CO ₂ Reduction. ACS Catalysis, 2022, 12, 8676-8686.	11.2	16

#	Article	IF	CITATIONS
181	Enhanced activity of CuO/K ₂ CO ₃ /MgAl ₂ O ₄ catalyst for lean NO _x storage and reduction at high temperatures. RSC Advances, 2017, 7, 27405-27414.	3.6	15
182	Stabilization of layered manganese oxide by substitutional cation doping. Journal of Materials Chemistry A, 2019, 7, 7118-7127.	10.3	14
183	Single-atom Ru catalyst for selective synthesis of 3-pentanone <i>via</i> ethylene hydroformylation. Green Chemistry, 2021, 23, 9038-9047.	9.0	14
184	Efficient Hydrogenation of Alkyl Formate to Methanol over Nanocomposite Copper/Alumina Catalysts. ChemCatChem, 2014, 6, 3075-3079.	3.7	13
185	Investigating microstructure of Longmaxi shale in Shizhu area, Sichuan Basin, by optical microscopy, scanning electron microscopy and micro-computed tomography. Nuclear Science and Techniques/Hewuli, 2017, 28, 1.	3.4	13
186	Preparation and regeneration of supported single-Ir-site catalysts by nanoparticle dispersion via CO and nascent I radicals. Journal of Catalysis, 2020, 382, 347-357.	6.2	13
187	Sulfur-Promoted Hydrocarboxylation of Olefins on Heterogeneous Single-Rh-Site Catalysts. ACS Catalysis, 2022, 12, 4203-4215.	11.2	13
188	Quantitative Zn speciation in zinc-containing steelmaking wastes by X-ray absorption spectroscopy. Journal of Analytical Atomic Spectrometry, 2012, 27, 1667.	3.0	12
189	Photoelectron spectroscopy study of the electronic structures at CoPc/Bi(111) interface. Surface Science, 2017, 661, 34-41.	1.9	12
190	Nâ€Modified NiO Surface for Superior Alkaline Hydrogen Evolution. ChemSusChem, 2018, 11, 1020-1024.	6.8	12
191	Epitaxial Growth of Free-Standing Bismuth Film on Graphene Embedded with Nontrivial Properties. ACS Applied Electronic Materials, 2019, 1, 1817-1824.	4.3	12
192	Electronic structures of ultra-thin tellurium nanoribbons. Nanoscale, 2019, 11, 14134-14140.	5.6	12
193	An Engineered Superhydrophilic/Superaerophobic Electrocatalyst Composed of the Supported CoMoS _{<i>x</i>} Chalcogel for Overall Water Splitting. Angewandte Chemie, 2020, 132, 1676-1682.	2.0	12
194	Pt ₂ Cl ₈ ^{2–} Dimer Formation of [Bmim] ₂ PtCl ₄ Ionic Liquid When Confined in Silica Nanopores. Journal of Physical Chemistry C, 2014, 118, 3140-3144.	3.1	11
195	Insights into the Coordination and Extraction of Yttrium(III) Ions with a Phenoxyacetic Acid Ionicâ€Liquid Extractant. European Journal of Inorganic Chemistry, 2017, 2017, 2332-2339.	2.0	11
196	Local structural evolutions of CuO/ZnO/Al2O3 catalyst for methanol synthesis under operando conditions studied by in situ quick X-ray absorption spectroscopy. Nuclear Science and Techniques/Hewuli, 2017, 28, 1.	3.4	11
197	Structural Transformation of 2,7â€Dibromopyrene on Au(111) Mediated by Halogenâ€Bonding Motifs. ChemPhysChem, 2019, 20, 2376-2381.	2.1	10
198	Tuning the interfaces of Co–Co2C with sodium and its relation to the higher alcohol production in Fischer–Tropsch synthesis. Journal of Materials Science, 2020, 55, 9037-9047.	3.7	10

#	Article	IF	CITATIONS
199	XAFS and SRGI-XRD studies of the local structure of tellurium corrosion of Ni–18%Cr alloy. Nuclear Science and Techniques/Hewuli, 2019, 30, 1.	3.4	9
200	Direct and Efficient Synthesis of Clean H ₂ O ₂ from CO-Assisted Aqueous O ₂ Reduction. ACS Catalysis, 2020, 10, 13993-14005.	11.2	9
201	Initiating Ullmann-like coupling of Br2Py by a semimetal surface. Scientific Reports, 2021, 11, 3414.	3.3	9
202	COâ€Tolerant PEMFC Anodes Enabled by Synergistic Catalysis between Iridium Singleâ€Atom Sites and Nanoparticles. Angewandte Chemie, 2021, 133, 26381.	2.0	9
203	A Universal Singleâ€Atom Coating Strategy Based on Tannic Acid Chemistry for Multifunctional Heterogeneous Catalysis. Angewandte Chemie, 2022, 134, .	2.0	9
204	Pt-O4 moiety induced electron localization toward In2O-Triggered acetylene Semi-Hydrogenation. Journal of Catalysis, 2022, 407, 290-299.	6.2	9
205	Facet-Induced Strong Metal Chlorideâ``Support Interaction over CuCl ₂ /l³-Al ₂ O ₃ Catalyst to Enhance Ethylene Oxychlorination Performance. ACS Catalysis, 2022, 12, 8027-8037.	11.2	9
206	Adsorption characteristics of Cr (III) onto starchâ€graftâ€poly(acrylic acid)/organoâ€modifed zeolite 4A composite: A novel path to the adsorption mechanisms. Polymer Composites, 2018, 39, 1223-1233.	4.6	8
207	Emerging Characterizing Techniques in the Fine Structure Observation of Metal Halide Perovskite Crystal. Crystals, 2018, 8, 232.	2.2	8
208	Uranium-Induced Changes in Crystal-Field and Covalency Effects of Th4+ in Th1–xUxO2 Mixed Oxides Probed by High-Resolution X-ray Absorption Spectroscopy. Inorganic Chemistry, 2018, 57, 11404-11413.	4.0	8
209	Effects of cobalt carbide on Fischer–Tropsch synthesis with MnO supported Co-based catalysts. Journal of Energy Chemistry, 2020, 42, 227-232.	12.9	8
210	Distribution of Spin Density on Phenoxyl Radicals Affects the Selectivity of Aerobic Oxygenation of Phenols. Inorganic Chemistry, 2020, 59, 3562-3569.	4.0	8
211	In Situ X-ray Absorption Near-Edge Structure Calculation and Machine Learning Analysis of the Structural Evolution in Lithium-Ion Battery Cathode Materials. Journal of Physical Chemistry C, 2021, 125, 18979-18987.	3.1	8
212	Enhanced dissociation activation of CO2 on the Bi/Cu(1 1 1) interface by the synergistic effect. Journal of Catalysis, 2022, 410, 1-9.	6.2	8
213	Carbon-encapsulated metallic Co nanoparticles for Fischer-Tropsch to olefins with low CO2 selectivity. Applied Catalysis B: Environmental, 2022, 316, 121700.	20.2	8
214	Insights into the Electrochemical Reaction Mechanism of a Novel Cathode Material CuNi ₂ (PO ₄) ₂ /C for Li-Ion Batteries. ACS Applied Materials & Interfaces, 2018, 10, 3522-3529.	8.0	7
215	Constructing Mononuclear Palladium Catalysts by Precoordination/Solvothermal Polymerization: Recyclable Catalyst for Regioselective Oxidative Heck Reactions. Angewandte Chemie, 2019, 131, 2470-2475.	2.0	7
216	Ni Hollow Fiber Encapsulated Bi@Zeolite for Efficient CO ₂ Electroreduction. ACS Applied Energy Materials, 2021, 4, 8933-8940.	5.1	7

#	Article	IF	CITATIONS
217	Recent Progress with In Situ Characterization of Interfacial Structures under a Solid–Gas Atmosphere by HP-STM and AP-XPS. Materials, 2019, 12, 3674.	2.9	6
218	Microstructure Evolution of a Co/MnO Catalyst for Fischerâ€Tropsch Synthesis Revealed by <i>In Situ</i> XAFS Studies. ChemCatChem, 2019, 11, 2187-2194.	3.7	5
219	A wavelengthâ€dispersive Xâ€ray spectrometer for in/ex situ resonant inelastic Xâ€ray scattering studies. X-Ray Spectrometry, 2020, 49, 251-259.	1.4	5
220	Frontispiece: Subnanometer Bimetallic Platinum–Zinc Clusters in Zeolites for Propane Dehydrogenation. Angewandte Chemie - International Edition, 2020, 59, .	13.8	5
221	A novel self-assembly approach for synthesizing nanofiber aerogel supported platinum single atoms. Journal of Materials Chemistry A, 2020, 8, 15094-15102.	10.3	5
222	Highly Ethylene‧elective Electrocatalytic CO ₂ Reduction Enabled by Isolated Cuâ^'S Motifs in Metal–Organic Framework Based Precatalysts. Angewandte Chemie, 2022, 134, .	2.0	5
223	Design of wide-range energy material beamline at the Shanghai Synchrotron Radiation Facility. Nuclear Science and Techniques/Hewuli, 2018, 29, 1.	3.4	4
224	Electrochemical and Spectroscopic Study of Homo―and Heteroâ€Dimetallic Phthalocyanines as Catalysts for the Oxygen Reduction Reaction in Acidic Media. ChemElectroChem, 2018, 5, 3478-3485.	3.4	4
225	Oneâ€Pot Synthesis of a Highly Active 3â€Dimensional Feâ^'N _x â^'CNTs/rGO Composite Catalyst for Oxygen Reduction. ChemElectroChem, 2019, 6, 504-513.	3.4	4
226	Interfacial Proton Transfer for Hydrogen Evolution at the Sub-Nanometric Platinum/Electrolyte Interface. ACS Applied Materials & Interfaces, 2021, 13, 47252-47261.	8.0	4
227	Exploring the CO2 reduction reaction mechanism on Pt/TiO2 with the ambient-pressure X-ray photoelectron spectroscopy. Applied Surface Science, 2021, 568, 150933.	6.1	4
228	Property variation of ionic liquid [Bmim][AuCl4] immobilized on carboxylated polystyrene submicrospheres with a small surface area. Science Bulletin, 2013, 58, 2950-2955.	1.7	3
229	Research Progress on the Indirect Hydrogenation of Carbon Dioxide to Methanol. ChemSusChem, 2016, 9, 315-315.	6.8	3
230	Xâ€ray absorption spectroscopy study of synthetic cobalt blue pigments similar to Kangxi blue and white porcelain. Journal of the American Ceramic Society, 2018, 101, 2130-2136.	3.8	3
231	Grain-boundary corrosion of nickel-based alloy by synchrotron radiation technology. Surface Innovations, 2019, 7, 278-283.	2.3	3
232	Revealing the Adsorption and Decomposition of EP-PTCDI on a Cerium Oxide Surface. ACS Omega, 2019, 4, 17939-17946.	3.5	3
233	Direct Synthesis of Semimetal Phthalocyanines on a Surface with Insights into Interfacial Properties. Journal of Physical Chemistry C, 2020, 124, 8247-8256.	3.1	3
234	Boosting Photocatalytic Water Oxidation Over Bifunctional Rh 0 â€Rh 3+ Sites. Angewandte Chemie, 2021, 133, 22943.	2.0	2

#	Article	IF	CITATIONS
235	Ru ions enhancing the interface bonding between the Pt nanoparticle catalyst and perovskite support for super anti-sintering performance. Journal of Materials Chemistry A, 2022, 10, 8227-8237.	10.3	2
236	Tandem Catalysis for Selective Oxidation of Methane to Oxygenates Using Oxygen over PdCu/Zeolite. Angewandte Chemie, 2022, 134, .	2.0	2
237	Unveiling orbital coupling at the CoPc/Bi(111) surface by ab initio calculations and photoemission spectroscopy. RSC Advances, 2017, 7, 52143-52150.	3.6	1
238	Benzyl-rich ligand engineering of the photostability of atomically precise gold nanoclusters. Chemical Communications, 2022, , .	4.1	1
239	Frontispiz: Subnanometer Bimetallic Platinum–Zinc Clusters in Zeolites for Propane Dehydrogenation. Angewandte Chemie, 2020, 132, .	2.0	Ο
240	Innenrücktitelbild: Boosting Photocatalytic Water Oxidation Over Bifunctional Rh ⁰ â€Rh ³⁺ Sites (Angew. Chem. 42/2021). Angewandte Chemie, 2021, 133, 23211-23211.	2.0	0